Ryanodine Receptor–Mediated Calcium Leak Drives Progressive Development of an Atrial Fibrillation Substrate in a Transgenic Mouse Model

Na Li, David Y. Chiang, Sufen Wang, Qiongling Wang, Liang Sun, Niels Voigt, Jonathan L. Respress, Sameer Ather, Darlene G. Skapura, Valerie K. Jordan, Frank T. Horrigan, Wilhelm Schmitz, Frank U. Müller, Miguel Valderrabano, Stanley Nattel, Dobromir Dobrev and Xander H.T. Wehrens

Circulation. 2014;129:1276-1285; originally published online January 7, 2014;
doi: 10.1161/CIRCULATIONAHA.113.006611
Circulation is published by the American Heart Association, 7272 Greenville Avenue, Dallas, TX 75231

Print ISSN: 0009-7322. Online ISSN: 1524-4539

Ryanodine Receptor–Mediated Calcium Leak Drives Progressive Development of an Atrial Fibrillation Substrate in a Transgenic Mouse Model

Na Li, PhD*; David Y. Chiang, BS*; Sufen Wang, PhD; Qiongling Wang, PhD; Liang Sun, PhD; Niels Voigt, MD; Jonathan L. Respress, PhD; Sameer Ather, MD, PhD; Darlene G. Skapura, BS; Valerie K. Jordan, BS; Frank T. Horrigan, PhD; Wilhelm Schmitz, MD; Frank U. Müller, MD; Miguel Valderrabano, MD; Stanley Nattel, MD; Dobromir Dobrev, MD; Xander H.T. Wehrens, MD, PhD

Background—The progression of atrial fibrillation (AF) from paroxysmal to persistent forms remains a major clinical challenge. Abnormal sarcoplasmic reticulum (SR) Ca^{2+} leak via the ryanodine receptor type 2 (RyR2) has been observed as a source of ectopic activity in various AF models. However, its potential role in progression to long-lasting spontaneous AF (sAF) has never been tested. This study was designed to test the hypothesis that enhanced RyR2-mediated Ca^{2+} release underlies the development of a substrate for sAF and to elucidate the underlying mechanisms.

Methods and Results—CREM-IbΔC-X transgenic (CREM) mice developed age-dependent progression from spontaneous atrial ectopy to paroxysmal and eventually long-lasting AF. The development of sAF in CREM mice was preceded by enhanced diastolic Ca^{2+} release, atrial enlargement, and marked conduction abnormalities. Genetic inhibition of Ca^{2+}/calmodulin-dependent protein kinase II–mediated RyR2-S2814 phosphorylation in CREM mice normalized open probability of RyR2 channels and SR Ca^{2+} release, delayed the development of spontaneous atrial ectopy, fully prevented sAF, suppressed atrial dilation, and forestalled atrial conduction abnormalities. Hyperactive RyR2 channels directly stimulated the Ca^{2+}-dependent hypertrophic pathway nuclear factor of activated T cell/Rcan1-4, suggesting a role for the nuclear factor of activated T cell/Rcan1-4 system in the development of a substrate for long-lasting AF in CREM mice.

Conclusions—RyR2-mediated SR Ca^{2+} leak directly underlies the development of a substrate for sAF in CREM mice, the first demonstration of a molecular mechanism underlying AF progression and sAF substrate development in an experimental model. Our work demonstrates that the role of abnormal diastolic Ca^{2+} release in AF may not be restricted to the generation of atrial ectopy but extends to the development of atrial remodeling underlying the AF substrate. **(*Circulation*. 2014;129:1276-1285.)**

Key Words: atrial fibrillation ■ calcium ■ mice ■ ryanodine receptor calcium release channel

Atrial fibrillation (AF) represents the most common sustained cardiac arrhythmia and is projected to increase considerably by 2050.[1] One of the most striking yet least understood characteristics of AF is its progressive nature. Patients often show spontaneous atrial ectopy before manifesting clinical AF, which may progress from a paroxysmal form to chronic and persistent states associated with significant morbidity and mortality.[2] Clinically, the risk factors for AF progression remain elusive, although the $CHADS_2$ score appears to be useful in predicting which patients progress to more advanced persistent AF forms during antiarrhythmic drug therapy.[3] However, despite advances in AF treatment, there is still no effective therapeutic strategy for the prevention of AF recurrences and progression.

Clinical Perspective on p 1285

Although there is hope that improved understanding of the molecular mechanisms underlying AF progression can lead to more effective therapeutic strategies,[2] the mechanisms underlying the progression from spontaneous atrial

Received June 7, 2013; accepted December 26, 2013.

From the Cardiovascular Research Institute, Department of Molecular Physiology & Biophysics (N.L., D.Y.C., L.S., J.L.R., S.A., D.G.S., V.K.J., F.T.H., X.H.T.W.), Translational Biology and Molecular Medicine Program (D.Y.C.), and Department of Medicine, Cardiology (X.H.T.W.), Baylor College of Medicine, Houston, TX; Department of Cardiology, The Methodist Hospital, Houston, TX (S.W., M.V.); Institute of Pharmacology, Faculty of Medicine, University Duisburg-Essen, Essen, Germany (N.V., D.D.); Division of Experimental Cardiology, Heidelberg University, Mannheim, Germany (N.V., D.D.); Institute of Pharmacology and Toxicology, University of Münster, Münster, Germany (W.S., F.U.M.); and Department of Medicine, Montreal Heart Institute and Université de Montréal, QC, Canada (S.N.).

*Dr Li and D.Y. Chiang contributed equally.

The online-only Data Supplement is available with this article at http://circ.ahajournals.org/lookup/suppl/doi:10.1161/CIRCULATIONAHA.113.006611/-/DC1.

Correspondence to Xander H.T. Wehrens, MD, PhD, Baylor College of Medicine, One Baylor Plaza, BCM335 Houston, TX 77030. E-mail wehrens@bcm.edu

ectopy to spontaneous AF (sAF) remain poorly understood. The transgenic mouse model of cardiac overexpression of transcriptional repressor CREM-IbΔC-X (CREM) is the first experimental model of which we are aware that recapitulates the typical pattern of AF progression seen in patients.[4] Telemetry ECG recordings demonstrated that CREM mice first exhibit spontaneous atrial ectopy by the age of 3 months, followed by the development of paroxysmal AF (pAF) and eventually persistent AF.

Enhanced activity of the sarcoplasmic reticulum (SR) Ca^{2+} release channel, also known as the type 2 ryanodine receptor channel (RyR2), has been implicated as one of the major mechanisms of cellular afterdepolarizations and triggered activity, an important mechanism underlying proarrhythmic ectopic activity in the heart.[2,5,6] An important cause of enhanced RyR2 Ca^{2+} leak is RyR2 hyperphosphorylation.[2,5,7] Increased Ca^{2+}/calmodulin-dependent protein kinase II (CaMKII) activity and enhanced serine-2814 (S2814) phosphorylation of RyR2 are detected in patients with long-lasting persistent AF.[5,7,8] Moreover, increased S2814 phosphorylation on RyR2 increases the susceptibility to AF induction by programmed electric stimulation in mutant mouse models.[7] However, it is not known whether RyR2 dysfunction caused by channel hyperphosphorylation contributes to AF progression and whether this represents an important contributor to the development of sAF.

Here, we tested the hypothesis that enhanced SR Ca^{2+} release resulting from increased phosphorylation of S2814 on RyR2 promotes the progression from atrial ectopy to pAF and persistent AF in CREM mice. Our data revealed that phosphorylation of S2814 on RyR2 is augmented before the onset of sAF, genetic inhibition of S2814 phosphorylation of RyR2 delays the onset of atrial ectopy and prevents the development of sAF in CREM mice, and normalization of RyR2-mediated SR Ca^{2+} release prevents atrial dilatation and atrial conduction abnormalities associated with the development of AF maintenance. Together, these findings suggest that the phosphorylation state of RyR2 may be a central motif in AF progression and that preventing RyR2 hyperphosphorylation may be a novel and effective strategy to prevent more advanced forms of AF.

Methods

Experimental Animals

Mouse studies were performed according to Institutional Animal Care and Use Committee–approved protocols. CREM transgenic mice (FVB/N background) and RyR2-S2814A mice (C57Bl/6 background) were interbred, and mice on a mixed background were used.[5]

Telemetry ECG

Mice were implanted with telemeters as previously described.[9]

Intracardiac Electrophysiology in Mice

In vivo electrophysiology studies were performed in mice at the age of 4 to 5 months, as described elsewhere.[7]

Myocyte Calcium Imaging

Atrial myocytes were isolated by a modified collagenase method as described.[7] Fluo-4-AM–loaded myocytes were imaged with confocal microscopy, and SR Ca^{2+} content was measured with a caffeine application.[7]

Single RyR2 Recordings

Single-channel recordings were obtained under voltage-clamp conditions, as described previously.[8]

Optical Mapping

Optical mapping of action potentials in the mouse atria was performed in mice at the age of 3 to 5 months, as described elsewhere.[5]

Western Blotting

Western blot analysis was performed in atrial samples of study animals at the ages of 1 month (no atrial arrhythmias), 3 months (atrial ectopy before the onset of sAF), and 7 months (long-lasting sAF).[5]

Human Atrial Samples

Human atrial samples were obtained with patients' consent and approval of the Institutional Review Board of the Medical Faculty Mannheim-Heidelberg University. Patient characteristics are provided in Table I in the online-only Data Supplement.

Results

Properties of the Model

CREM mice began to exhibit atrial ectopy at ~3 months of age (Figure 1A). Quantification of atrial ectopic activity revealed a higher incidence of atrial ectopic beats (3.0±0.7 beats per hour) in 3-month-old CREM mice compared with wild-type (WT) mice, none of which exhibited atrial ectopic beats (Figure 1B). By 5 months of age, all of the CREM mice showed ectopy (2.9±0.7 beats per hour), and 38% of the CREM mice (5 of 13) showed at least 1 episode of sAF at this age. The average duration of the longest sAF episode was 32.6±14.4 minutes (Figure 1C). By 7 months, >77% of CREM mice (17 of 22) had developed many and long-lasting episodes of sAF (Figure 1D). CREM mice were in sAF for 52±10% of the recording time, much more than 5-month-old CREM mice (9.0±5.3%; $P<0.05$). More strikingly, the average duration of the longest episode of sAF in each animal was greatly prolonged, to 493.6±154.9 minutes ($P<0.05$ versus 5-month-old CREM mice). In contrast, none of the WT mice developed sAF by 5 or 7 months of age.

From previous work, we anticipated that CaMKII activity might be enhanced in CREM mice.[4,5] Figure 2A shows that CaMKII autophosphorylation at T287 indeed progressively increased with age (Figure 2A). Total CaMKII protein levels in CREM mice, however, were reduced to 32±6% of those in WT mice at 7 months of age. These changes in CaMKII expression and autophosphorylation levels were associated with a progressive increase in RyR2 phosphorylation at the CaMKII phosphorylation site S2814 starting at 3 months of age and further increasing by 7 months of age (Figure 2B). Another downstream target of CaMKII in the SR is threonine 17 of phospholamban, which was unchanged in CREM mice (Figure 2C). This suggests that RyR2 hyperphosphorylation at S2814 might not result only from increased global CaMKII autophosphorylation. On the other hand, phosphorylation of RyR2-S2808, which is regulated primarily by protein kinase A, was also unaltered in CREM mice (Figure 2D).

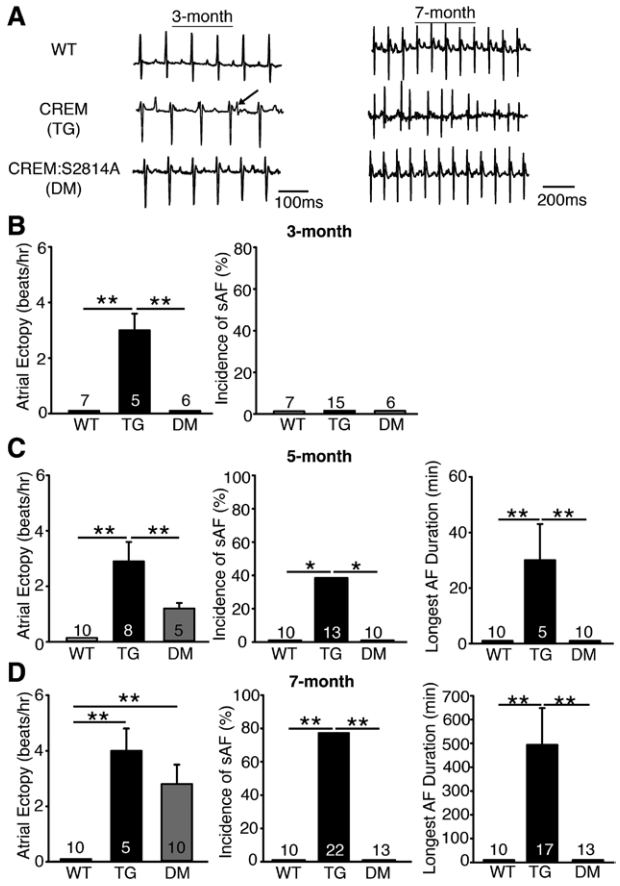

Figure 1. Progression of atrial arrhythmia in CREM-IbΔC-X transgenic (CREM; TG) and CREM:S2814A (DM) mice. **A**, Representative telemetry ECG recordings revealed the presence of spontaneous atrial ectopy at the age of 3 months and the presence of spontaneous atrial fibrillation (sAF) at the age of 7 months in CREM mice, whereas no AF was observed in wild-type (WT) or CREM:S2814A mice. **B**, **Left**, The number of atrial ectopic events in mice that exhibited sinus rhythm at the age of 3 months. **Right**, The incidence of sAF at the age of 3 months. **C** and **D**, **Left**, The number of atrial ectopic events in mice that exhibited atrial ectopy at the age of 5 and 7 months. **Middle**, The incidence of sAF at the age of 5 and 7 months. **Right**, The duration of longest episodes of sAF at the age of 5 and 7 months. Numbers in the bars indicate the number of animals studied. **P*<0.05; ***P*<0.01.

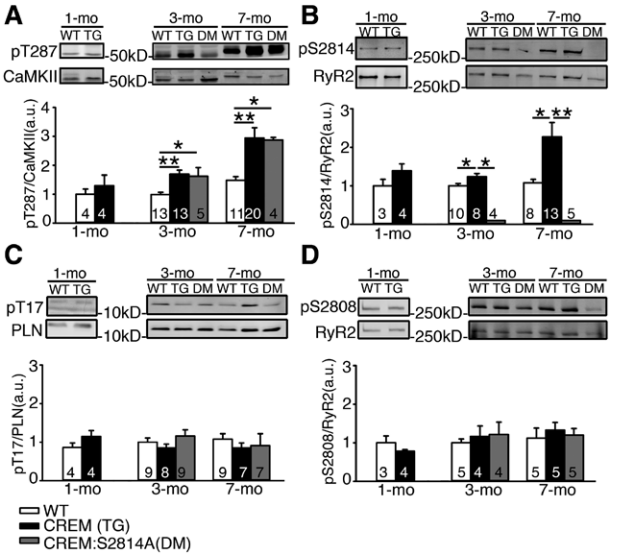

Figure 2. Ca^{2+}/calmodulin-dependent protein kinase II (CaMKII) phosphorylation of ryanodine receptor type 2 (RyR2) in CREM-IbΔC-X transgenic (CREM; TG) mice increases before the onset of spontaneous atrial fibrillation. **A**, Western blots showing age-dependent increase in the level of T287 autophosphorylation normalized to total CaMKII levels. **B**, Western blots showing progressive increase in the level of S2814 phosphorylation normalized to total RyR2 levels. **C**, Western blots showing the level of threonine 17 phosphorylation normalized to total phospholamban levels. **D**, Western blots showing the level of S2808 phosphorylation normalized to total RyR2 levels. Numbers in the bars indicate the number of animals studied. WT indicates wild-type. **P*<0.05; ***P*<0.01.

CaMKII hyperphosphorylation of RyR2 can enhance SR Ca^{2+} release in cardiomyocytes. Therefore, we measured diastolic SR Ca^{2+} leak using standard methodology,[10] as illustrated in Figure 3A. SR Ca^{2+} leak was enhanced in CREM mice at the age of 7 months (Figure 3A and 3B). Enhanced SR Ca^{2+} leak can reduce SR Ca^{2+} content, which was shown in CREM mouse atrial cardiomyocytes (Figure 3C). To determine whether increased CaMKII activity contributes to abnormal RyR2-mediated SR Ca^{2+} release, SR Ca^{2+} leak was evaluated in cells pretreated with the CaMKII inhibitor KN-93 for 30 minutes. Inhibition of CaMKII normalized both SR Ca^{2+} leak and SR Ca^{2+} load in CREM mice to levels similar to those seen in WT mice (Figure 3B and 3C). Although these data point to a role for CaMKII hyperphosphorylation of RyR2 at S2814, the pharmacological agent KN-93 inhibits CaMKII generally. To better pinpoint the mechanism of action, we used a genetic model in which S2814 phosphorylation is prevented by a serine-to-alanine mutation (S2814A) to assess specifically the role of this CaMKII phosphorylation site.

Genetic Inhibition of CaMKII Phosphorylation of RyR2 Reduces SR Ca^{2+} Leak in CREM Mice

First, we tested whether inhibition of RyR2 phosphorylation at S2814 could normalize SR Ca^{2+} release defects caused by CREM overexpression. Ca^{2+} spark frequency was measured in atrial cardiomyocytes from WT, CREM, and CREM:S2814A mice. Consistent with previous studies,[4] Ca^{2+} spark frequency was significantly higher in CREM mice (5.3±0.9 sparks/100μm/s) than in WT littermates (2.0±0.3 sparks/100μm/s; *P*<0.05; Figure 4A and 4B). Pretreating cells with the CaMKII inhibitor KN-93 (1 μmol/L) reduced Ca^{2+} spark frequency (Figure 4A and 4B), consistent with its effects on SR Ca^{2+} leak (Figure 3), whereas the inactive control KN-92 (1 μmol/L) was without effect (Figure 4B). Consistently, autocamtide-2–related inhibitory peptide (AIP, 1 μmol/L), a CaMKII inhibitor with better specificity than KN-93, also reduced Ca^{2+} spark frequency in CREM mice (*P*<0.05 versus CREM; Figure 4B). Moreover, genetic inhibition of RyR2 phosphorylation at S2814 in the CREM:S2814A mice also reduced Ca^{2+} spark frequency (2.1±0.4 sparks per 100 μm per second; *P*<0.05 versus CREM; Figure 4A and 4B) and reversed other Ca^{2+} spark abnormalities observed in CREM mice such as prolonged duration and slowed decay times (ie, prolonged τ; Table II in the online-only Data Supplement). Together, these findings suggest that CaMKII phosphorylation of

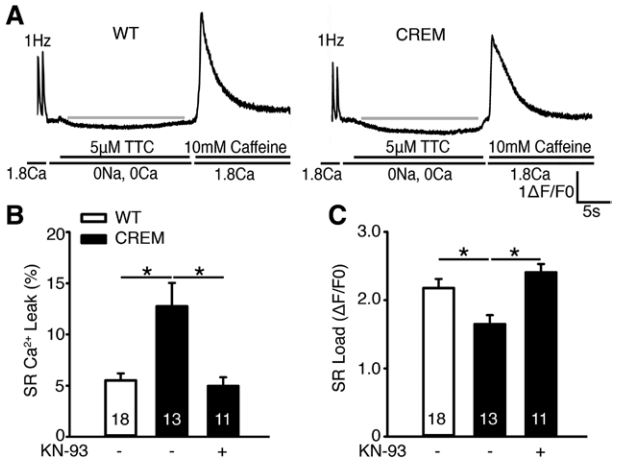

Figure 3. Inhibition of Ca^{2+}/calmodulin-dependent protein kinase II (CaMKII) reduces sarcoplasmic reticulum (SR) Ca^{2+} leak in CREM-IbΔC-X transgenic (CREM) mice. **A**, Representative $[Ca^{2+}]_i$ tracings from atrial myocytes paced at 1 Hz followed by a rapid switch to Tyrode solution containing 0 Na^+, 0 Ca^{2+}, and 5 μmol/L tetracaine (TTC) to block ryanodine receptor type 2–mediated SR Ca^{2+} leak. To measure SR Ca^{2+} content, 10 mmol/L caffeine was added. At the age of 7 months, CREM mice exhibited increased SR Ca^{2+} leak, measured as the curve below the grey baseline. **B**, Quantification of SR Ca^{2+} leak normalized to SR Ca^{2+} load revealed that increased leak in CREM mice was normalized by CaMKII inhibition with KN-93. **C**, Bar graph showing reduced SR Ca^{2+} load in CREM mice, which was normalized with KN-93. Numbers in the bars indicate the number of cells studied from 3 to 4 animals. WT indicates wild-type. *P<0.05.

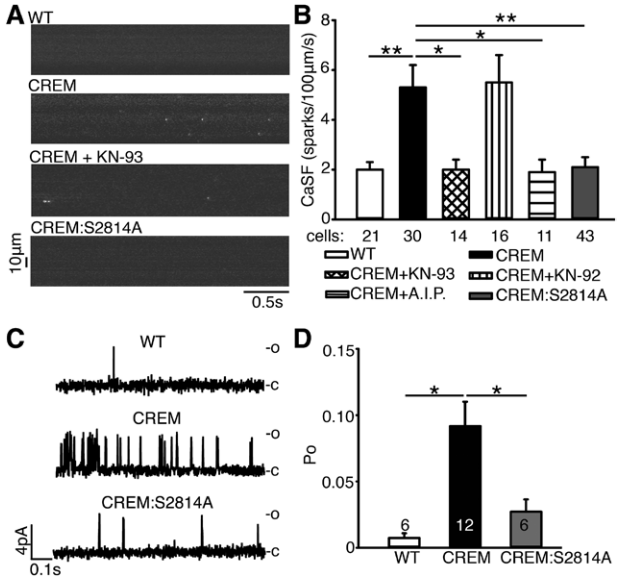

Figure 4. Genetic inhibition of S2814 phosphorylation on ryanodine receptor type 2 (RyR2) normalizes RyR2 activity in CREM-IbΔC-X transgenic (CREM) mice. **A**, Line-scan confocal images of atrial myocytes revealed more spontaneous Ca^{2+} sparks in CREM mice. **B**, Ca^{2+} spark frequency (CaSF). **C**, RyR2 single-channel recordings revealed more openings (o) as shown upward deflections from the closed (c) level in CREM mice. **D**, Open probability (Po) of RyR2 channels. Numbers in the bars indicate the number of cells/channels studied from 3 to 4 mice. WT indicates wild-type. *P<0.05.

RyR2 is a critical mechanism in terms of causing SR Ca^{2+} release defects.

RyR2 Channels Are Hyperactive in CREM Mice Before the Onset of sAF

To determine the function of RyR2 channels in CREM mice before the onset of sAF, we studied the single-channel properties of RyR2 channels obtained from atrial tissues of WT, CREM, and CREM:S2814A mice at the age of 3 months (Figure 4C). The RyR2 channels exhibited higher open probability (Po) in CREM mice (0.092±0.018) than in WT mice (0.0074±0.0036; P<0.05). Genetic inhibition of RyR2 phosphorylation in CREM:S2814A mice reduced Po to 0.027±0.009 (P<0.05 versus CREM; Figure 4D). These findings suggest that RyR2 channels are hyperactive in CREM mice, whereas hyperactivity was prevented by the S2814A mutation.

Inhibition of RyR2 Ca^{2+} Leak Prevents Progression to sAF in CREM Mice

To evaluate the impact of RyR2-mediated Ca^{2+} release on spontaneous atrial arrhythmogenesis in CREM mice, we performed 24-hour telemetry recordings in CREM:S2814A mice. Unlike CREM mice, none of the CREM:S2814A mice exhibited atrial ectopy at 3 months of age (Figure 1B). By 5 months, none of the CREM:S2814A mice had developed sAF, although a few exhibited spontaneous atrial ectopic events (Figure 1C). Moreover, by 7 months, none of the CREM:S2814A mice had progressed to sAF, whereas 77% of the CREM mice exhibited prolonged sAF episodes (Figure 1D). The bar graph in Figure I in the online-only Data Supplement summarizes the incidence of spontaneous atrial ectopy and sAF in WT, CREM, and CREM:S2814A mice at 3 different ages, suggesting that inhibition of S2814 phosphorylation on RyR2 delays the onset of spontaneous atrial ectopy and, more important, prevents its progression to sAF.

Inhibition of RyR2 Ca^{2+} Leak Suppresses the Inducibility and Maintenance of AF in CREM Mice

By 5 months of age, all CREM mice (n=13) exhibited atrial ectopic activity, and 38.5% (5 of 13) also showed episodes of sAF. To evaluate whether S2814 phosphorylation plays a critical role in the substrate for AF, we performed programmed electric stimulation at this age (Figure 5). Programmed electric stimulation was performed at a time when the CREM mice did not yet exhibit sAF so that we could be sure that any AF episodes were indeed induced and not a spontaneous occurrence or continuation of preexisting AF. Whereas 54% of the CREM mice (7 of 13) developed reproducible AF after atrial burst pacing (defined as at least 2 of the 3 burst pacing protocols resulting in AF episodes lasting >1 second), only 1 of 12 WT (8.3%) and none of the 12 CREM:S2814A (0%) mice developed pacing-induced AF (Figure 5B). In addition, the average duration of the longest inducible AF episodes was longer in CREM mice compared with WT (P<0.05) and CREM:S2814A (P<0.05) mice (Figure 5C), suggesting that the S2814A mutation in RyR2 prevents the perpetuation of AF in CREM mice.

The increased likelihood of AF induction was not secondary to global changes in cardiac electrophysiology because there were no significant differences in cardiac electrophysiological parameters such as heart rate or QRS and QTc intervals among the different genotypes of mice (Table III in the

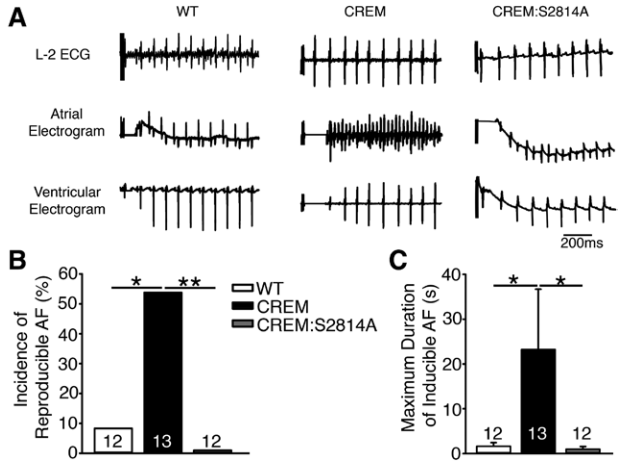

Figure 5. Genetic inhibition of S2814 phosphorylation on RyR2 suppresses the maintenance of atrial fibrillation (AF) in CREM-IbΔC-X transgenic (CREM) mice. **A**, Lead 2 (L2) ECG and intracardiac electrograms of pacing-induced AF in CREM mice at 5 months of age. **B**, Increased incidence of pacing-induced AF in CREM mice (n=12) at 5 months of age compared with wild-type (WT; n=10) and CREM:S2814A (n=12) mice. **C**, The average duration of the longest AF episode in each animal induced by pacing. *P<0.05.

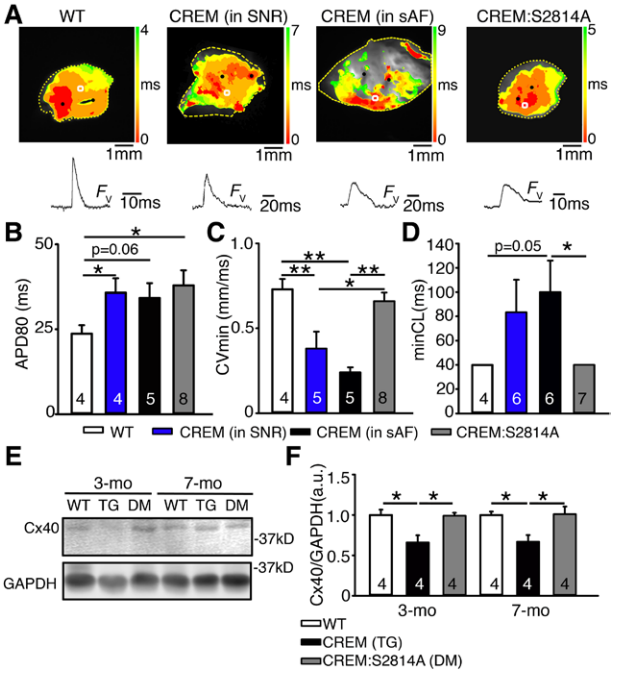

Figure 6. Improved conduction velocity and excitability in CREM:S2814A (DM) mice. **A**, **Top**, Activation map of isolated atria preparations obtained from 5-month-old mice. **Bottom**, Voltage fluorescence (F_v) traces obtained from the indicated regions (white squares). **B**, Action potential duration at 80% repolarization (APD_{80}), (**C**) minimum conduction velocity (CVmin), and (**D**) minimum cycle length (minCL) that can pace the atria. **E**, Western blots showing reduction in the level of Cx40 protein in CREM-IbΔC-X transgenic (CREM; TG) mice before and after the onset of sAF. **F**, Quantification of connexin40 (Cx40) protein level normalized to GAPDH. Numbers in the bars indicate the number of animals studied. sAF indicates spontaneous atrial fibrillation; SNR, normal sinus rhythm; and WT, wild-type. *P<0.05; **P<0.01.

online-only Data Supplement). However, the PR interval was significantly prolonged in CREM compared with WT mice but normalized in the CREM:S2814A mice (Table III in the online-only Data Supplement). Other parameters such as the corrected sinus node recovery time, atrial effective refractory period, and atrioventricular node effective refractory period were all unchanged in CREM mice compared with WT mice (Table III in the online-only Data Supplement). Finally, there were no significant changes in ventricular contractility and dimensions in 5-month-old CREM mice compared with WT mice (Table IV in the online-only Data Supplement), suggesting that the development of persistent AF is not caused by ventricular remodeling.

Inhibition of RyR2 Ca^{2+} Leak Improves Atrial Conduction and Excitability

To understand the PR prolongation and the AF substrate demonstrated by prolonged sAF and pacing-induced AF in CREM mice, we performed optical mapping on atrial tissue preparations isolated from 5-month-old mice. Surprisingly, we found that regardless of whether the CREM mice were in normal sinus rhythm or in sAF, all of them had developed electric remodeling at this age (Figure 6). First, atrial preparations from all CREM mice, both in sinus rhythm and with sAF, displayed biatrial enlargement with apparent loss of viable cardiomyocytes, as evidenced by large unexcitable areas in their atrial tissue (Figure 6A). Second, during 5-Hz pacing, CREM mice in both sinus rhythm (35.8±4.2 milliseconds) and sAF (34.2±4.4 milliseconds) exhibited prolonged atrial action potential duration at 80% repolarization (APD_{80}) compared with WT mice (23.7±2.5 milliseconds; P<0.05 versus CREM in sinus rhythm, P=0.06 versus CREM in sAF; Figure 6B). Moreover, the conduction velocity was significantly reduced in both CREM mice in sinus rhythm (0.38±0.10 mm/ms) and mice with sAF (0.24±0.03 mm/ms) compared with WT mice (0.73±0.06 mm/ms; P<0.01; Figure 6C). CREM mice also had a decreased ability to sustain rapid pacing rates, and the minimum pacing cycle length at which they captured was longer (83.3±26.8 milliseconds in sinus rhythm; 100±25.9 milliseconds in sAF) than in WT mice (40.0±0.0 milliseconds; P=0.05; Figure 6D). Although atrial preparations from CREM:S2814A mice still exhibited prolonged APD_{80} (38.0±4.4 milliseconds; P<0.05 versus WT), they showed normalized atrial dimensions, improved conduction velocity (0.66±0.05 mm/ms; P<0.05 versus CREM in sinus rhythm, P<0.01 versus CREM in sAF), and normalized minimum pacing cycle length (40.0±0.0 milliseconds; P<0.05 versus CREM in sinus rhythm; Figure 6A–6D). Because CREM mice developed clear electric remodeling without AF at a time when a minority of mice displayed sAF, the remodeling is clearly not secondary to AF.

To address the mechanism of APD prolongation in both CREM and CREM:S2814A mice, we measured L-type Ca^{2+} current ($I_{Ca,L}$) in isolated atrial myocytes. Our data revealed that $I_{Ca,L}$ was enhanced in both CREM and CREM:S2814A mice compared with WT mice (Figure II in the online-only Data Supplement), suggesting that the $I_{Ca,L}$ gain-of-function results from CREM overexpression independently of RyR2-mediated Ca^{2+} release.

Previously, we showed that the reduced conduction velocity in CREM mice is associated with a downregulation of

connexin (Cx) 40,[4] a major component of atrial gap junctions, whereas Cx43 expression is unaltered. To evaluate whether the improvement in conduction velocity in CREM:S2814A mice is related to a change in Cx40 expression, we quantified Cx40- protein by Western blotting. Consistent with optical mapping results, Cx40 expression was downregulated in CREM mice as early as 3 months of age ($P<0.05$ versus WT), before the onset of sAF (Figure 6E and 6F). Cx40 remained downregulated by 30% in CREM mice as they developed long-lasting persistent sAF ($P<0.05$ versus WT), consistent with previous observations.[4] However, Cx40 expression was restored in CREM:S2814A mice at both 3 and 7 months of age ($P<0.05$ versus CREM; Figure 6E and 6F). These findings suggest that RyR2-mediated SR Ca^{2+} leak may be involved in the downregulation of Cx40.

Inhibition of RyR2 Ca^{2+} Leak Attenuates Atrial Enlargement in CREM Mice

The continued presence of AF has been shown to induce atrial structural remodeling that further perpetuates AF in various large-animal models.[11,12] To determine whether inhibition of RyR2 Ca^{2+} leak alters structural remodeling associated with chronic AF (cAF), hearts were collected from 7-month-old mice. There was clear biatrial enlargement in CREM mice compared with WT and CREM:S2814A mice (Figure 7A). Quantification of the atrial weight normalized to tibia length revealed that the atrial mass was increased by 162% in CREM mice (2.05±0.43 mg/mm) compared with WT mice (0.41±0.08 mg/mm; $P<0.05$; Figure 7B). In contrast, the ratio of atrial weight to tibia length was normalized in CREM:S2814A mice (0.39±0.05 mg/mm; $P<0.05$ versus CREM). Quantification of the total heart weight normalized to tibia length did not reveal a significant increase in CREM mice (7.9±0.4 mg/mm) compared with WT mice (6.7±1.0 mg/mm) and CREM:S2814A mice (7.5±0.3 mg/mm). To evaluate whether the structural remodeling in the atria preceded the onset of sAF, we quantified the ratio of atrial weight to tibia length in 3-month-old mice. At this age, the ratio of atrial weight to tibia length was already significantly increased in CREM mice (1.5±0.3 mg/mm) compared with WT (0.26±0.03; $P<0.01$), but it was unchanged in CREM:S2814A mice (0.28±0.03 mg/mm; $P<0.01$ versus CREM; Figure III in the online-only Data Supplement). These data suggest that hypertrophic pathways are activated directly by RyR2-mediated Ca^{2+} leak and that atrial structural remodeling is not secondary to AF.

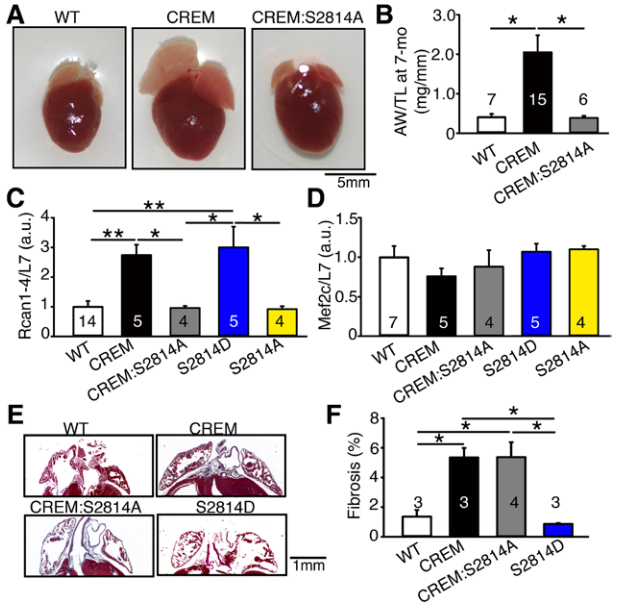

Figure 7. Reversal of atrial hypertrophy but maintenance of atrial fibrosis in CREM:S2814A mice. **A**, Whole-mount photographs of hearts from 7-month-old wild-type (WT), CREM-IbΔC-X transgenic (CREM), and CREM:S2814A mice. **B**, The atrial weight-to-tibia length ratio (AW/TL) of 7-month-old mice. **C**, The level of Rcan1-4 mRNA normalized to L7. **D**, The level of Mef2c mRNA normalized to L7. **E**, Masson trichrome staining of fibrosis in atrial sections. **F**, Quantification of atrial fibrosis. Numbers in the bars indicate the number of animals studied. **P*<0.05; ***P*<0.01.

To determine whether known Ca^{2+}-dependent hypertrophic signaling systems, namely the calcineurin–nuclear factor of activated T cell (NFAT)–Rcan and CaMKII–histone deacetylase–Mef2c pathways, are activated before the onset of sAF, we evaluated expression of Rcan1-4 and Mef2c mRNA in atrial tissues from 3-month-old mice. We found that Rcan1-4, but not Mef2c, was upregulated in CREM mice compared with WT ($P<0.01$; Figure 7C and 7D). Consistent with a causative role of Ca^{2+} leak in NFAT/Rcan1-4 activation, Rcan1-4 expression was normalized in CREM:S2814A mice ($P<0.05$ versus CREM; Figure 7C and 7D). To determine whether Rcan1-4 is directly activated by RyR2 Ca^{2+} leak, we studied RyR2-S2814D (S2814D) mice in which the S2814D mutation mimics hyperphosphorylation and predisposes mice to pacing-induced AF.[8] Rcan1-4 is also upregulated in S2814D mice, supporting the idea of direct RyR2-mediated activation of Rcan1-4 (Figure 7C). Similar to findings in CREM mice, CaMKII-dependent activation of the hypertrophic molecule Mef2c was not altered in either S2814D or S2814A mice (Figure 7D). Together, these data indicate that RyR2-mediated Ca^{2+} release results in activation of the calcineurin-NFAT-Rcan pathway and promotes structural remodeling.

Finally, the level of atrial fibrosis was examined using Masson trichrome staining of longitudinal cardiac sections (Figure 7E). Quantification of fibrosis revealed enhanced atrial fibrous tissue content in both CREM (5.5±0.6%) and CREM:S2814A (5.4±1.0%) mice compared with WT mice (1.4±0.4%; both $P<0.05$; Figure 7F). These data suggest that the prevention of cAF development in CREM:S2814A mice did not result from the inhibition of atrial fibrosis. In addition, both CREM (6.0±0.9%) and CREM:S2814A (7.2±1.7%) mice had more ventricular fibrosis than WT mice (1.1±0.3%; both $P<0.05$; Figure IV in the online-only Data Supplement). Consistent with the idea that fibrosis in CREM mice does not result from RyR2 hyperphosphorylation/Ca^{2+} leak, RyR2-phosphomimetic S2814D mice did not exhibit fibrosis in either atria (0.87±0.06%; Figure 7E and 7F) or ventricles (0.45±0.09%; Figure IV in the online-only Data Supplement). Therefore, it is likely that the fibrosis observed in CREM mice is a direct consequence of cardiac CREM overexpression and not a consequence of AF-associated remodeling or a RyR2 Ca^{2+} release–dependent process.

Increased Level of CREM-IbΔC-X in AF Patients

Consistent with the results we observed in CREM mice, Rcan1-4 mRNA was increased 2-fold in atrial samples from pAF patients compared with patients in sinus rhythm ($P<0.05$; Figure 8A). We also observed similar amounts of Rcan1-4 upregulation in atrial samples from cAF patients ($P<0.05$ versus patients in sinus rhythm; Figure 8B). Unlike Rcan1-4, the level of Mef2c was unaltered in atrial samples from pAF and cAF patients (Figure 8B). These results further confirmed our findings on the hypertrophic signaling pathway involved in atrial remodeling in CREM mice. Finally, we evaluated the mRNA expression of CREM-IbΔC-X in atrial biopsies from patients in sinus rhythm, pAF, and cAF. The expression of this transcriptional repressor CREM-IbΔC-X is increased almost 2-fold in atrial samples from pAF and cAF patients compared with separate sets of randomly chosen patients in sinus rhythm ($P<0.05$; Figure 8C), positioning CREM as a potential contributor to human AF pathophysiology.

Discussion

Our data show for the first time a direct causal role of RyR2-mediated SR Ca^{2+} leak in atrial structural remodeling, which is required for the development of the substrate underlying sAF in CREM transgenic mice. Specifically, increased CaMKII-mediated phosphorylation of RyR2 preceded the transition from atrial ectopy to sAF in CREM mice, a transition that mimics the progressive nature of AF observed in humans. Suppression of SR Ca^{2+} leak by genetic inhibition of RyR2 phosphorylation at S2814 completely prevented sAF. Moreover, our study demonstrated that normalization of RyR2-mediated Ca^{2+} leak prevented slowed atrial conduction and atrial dilatation in CREM mice. Thus, our findings uncovered an unanticipated role for RyR2-mediated Ca^{2+} leak in the progression to persistent AF forms.

New Insights From the CREM Transgenic Mouse Model of Persistent AF

Mouse models represent an important animal system in which molecular signaling events involved in the pathogenesis of cardiac disease can be elucidated. However, to date, few mouse models of sAF have been reported. Prior studies demonstrated that CREM-transgenic mice not only exhibit sAF but also show a gradual, age-dependent transition from atrial ectopy to pAF and long-lasting AF, thus mimicking the disease progression often seen in AF patients.[4] Indeed, CREM mice at 7 months were in AF >50% of the time, with longest episodes averaging almost 10 hours in each mouse. Although it is clearly difficult to know what AF duration in humans would correspond to 10 hours of continuous AF in the mouse, correction by life expectancy suggests that this may be equivalent to a few weeks of continuous AF in humans.[13] Similar to classic large-animal models of AF induced by tachycardiac pacing,[14,15] CREM mice recapitulate key features of the persistent AF substrate such as slowed conduction, atrial dilatation, and increased fibrous tissue content, hallmarks of structural remodeling that correlate with the severity and persistence of AF in patients.[2] Therefore, we took advantage of this mouse model to gain new insights into the molecular pathogenesis of AF.

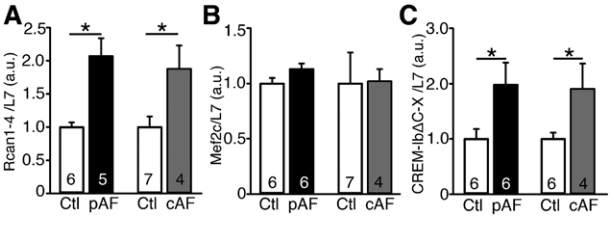

Figure 8. Upregulation of Rcan1-4 and CREM-IbΔC-X mRNA in atrial fibrillation (AF) patients. Level of Rcan1-4 (**A**), Mef2c (**B**), and CREM-IbΔC-X (**C**) mRNA normalized to L7 in atrial samples from patients. Independent experiments using separate sets of randomly chosen sinus rhythm (Ctl) samples were used to compare with paroxysmal AF (pAF) and chronic AF (cAF) samples. Numbers in the bars indicate the number of patients studied. *$P<0.05$.

CaMKII-Mediated Activation of RyR2 in AF

Previous studies have demonstrated that expression levels and activity of cytosolic CaMKII are upregulated in long-lasting persistent AF patients and in experimental AF models, including CREM mice.[5,8,16] CaMKII may be activated by the increased atrial rate or via enhanced oxidation of CaMKII.[17] CaMKII phosphorylation of RyR2 increases channel activity,[18] associated with increased SR Ca^{2+} leak, enhanced Ca^{2+} spark generation, and increased susceptibility to AF induction.[8] Conversely, genetic inhibition of RyR2 phosphorylation at S2814 prevents pacing-induced AF in mouse models with RyR2 defects.[5,7,8] Moreover, enhanced SR Ca^{2+} leak via defective RyR2 channels promotes atrial ectopic activity and promotes AF inducibility in several mouse models, including FKBP12.6-deficient mice[7,19] and mice heterozygous for catecholaminergic polymorphic ventricular tachycardia–associated RyR2 mutations.[5,20] These studies in mice and more recent work in atrial myocytes from patients with persistent AF demonstrated a mechanistic link between abnormal SR Ca^{2+} release events, activation of the Na^{+}-Ca^{2+} exchanger, and an increased likelihood of delayed afterdepolarizations and triggered activity that underlie atrial ectopic impulse formation.[8]

A previous study revealed that CREM transgenic mice exhibit increased SR Ca^{2+} leak as evidenced by an increased frequency of Ca^{2+} sparks and SR Ca^{2+} leak revealed by tetracaine exposure,[4] but the mechanisms underlying RyR2-mediated Ca^{2+} leak and its role in AF substrate development were not investigated. Here, we show that RyR2 hyperphosphorylation is clearly responsible for the hyperactive RyR2 channels in CREM transgenic mice because the enhanced open probability of RyR2 channels and the higher frequency of Ca^{2+} sparks were suppressed by inhibition of RyR2 phosphorylation in CREM:S2814A mice. Moreover, RyR2 hyperactivity is not attributable to enhanced phosphorylation levels of RyR2 at S2808, an important target for protein kinase A phosphorylation. In contrast, CaMKII phosphorylation of another key Ca^{2+} handling protein, phospholamban (at threonine 17), was also unchanged in CREM mice. A prior study by Greiser et al[21] also reported that only phosphorylation of S2814 on RyR2 is enhanced in 2 goat models of AF, whereas levels of S2808 phosphorylation and phospholamban–threonine 17 phosphorylation were unaltered. These findings suggest

that phosphorylation by CaMKII, but not protein kinase A, is responsible for RyR2 dysfunction in CREM mice. Because phospholamban was also not hyperphosphorylated by CaMKII, it is possible that altered regulation by protein phosphatases within the RyR2 complex may contribute to its differential phosphorylation.[22]

Mechanistic Link Between RyR2-Mediated SR Ca^{2+} Leak and Atrial Remodeling

Our data reveal that key components of atrial remodeling in CREM mice, in particular atrial dilatation and conduction slowing, are mediated by increased diastolic SR Ca^{2+} leak via RyR2. This conclusion is based on the observations that RyR2 activity is increased in CREM mice before the onset of sAF and that RyR2 single-channel activity is reduced to WT levels in CREM:S2814A mice. Moreover, CREM:S2814A mice were protected from developing atrial dilatation, conduction velocity slowing, and sAF. In contrast, other major contributors to atrial remodeling such as atrial fibrosis and altered APD were not normalized in CREM:S2814 mice, suggesting that these aspects of atrial remodeling occur independently of RyR2-mediated Ca^{2+} leak.

Our data suggest that the conduction slowing in CREM mice is caused at least in part by downregulation of Cx40, an important protein in atrial gap junctions.[4] Normalization of the Cx40 expression in CREM:S2814A mice suggests that the Cx40 downregulation may also be driven by RyR2-mediated Ca^{2+} leak. A recent study by King et al[23] also demonstrated slower interatrial conduction velocity in a mouse model of catecholaminergic polymorphic ventricular tachycardia, with a gain-of-function RyR2 mutation causing SR Ca^{2+} leak. Taken together, these findings suggest that RyR2 dysfunction may promote reentrant arrhythmogenesis by promoting the development of a susceptible substrate involving structural remodeling and Cx40 downregulation–mediated conduction slowing.[23]

In terms of potential mechanisms underlying structural remodeling, our data revealed that RyR2 mediated SR Ca^{2+} leak–dependent activation of the calcineurin-NFAT-Rcan pathway in both CREM transgenic mice and AF patients, whereas the CaMKII–histone deacetylase–Mef2c pathway was not affected. Interestingly, constitutive CaMKII phosphorylation of S2814, which is associated with enhanced RyR2 single-channel activity, was sufficient to activate the calcineurin-NFAT-Rcan pathway, suggesting a direct causal link between RyR2-mediated SR Ca^{2+} leak and structural remodeling.

Enhanced activation of the calcineurin-NFAT-Rcan pathway has been implicated in humans with AF and animal models of AF.[24] NFAT translocation regulates mRNA transcription, leading to remodeling of 2 key atrial ion channels, that is, downregulation of the α-subunit of $I_{Ca,L}$[25] and microRNA-26–mediated upregulation of the Kir2.1 subunit of the inward-rectifier K^+ channel (I_{K1}).[26] Augmentation of I_{K1} is an important AF maintenance factor because of its APD-shortening effect, leading to stabilization of rotors.[27] Our results suggest that the RyR2-mediated SR Ca^{2+} leak may be the key process that initiates both electric and structural atrial remodeling, promoting the transition from paroxysmal to persistent AF.

Frequent Atrial Ectopy Is Not Sufficient to Cause sAF in CREM Mice

It is often assumed that ectopic complexes precede AF because they manifest as a sustained tachyarrhythmic "driver" or trigger reentrant arrhythmia in a vulnerable substrate. Another possibility is that atrial ectopy can by itself induce atrial remodeling. The present findings suggest, however, that atrial ectopy is not sufficient to cause atrial remodeling associated with substrate development for sAF in CREM mice. Although CREM:S2814A mice eventually exhibited substantial atrial ectopy, they never developed spontaneous episodes of AF. The S2814A mutation in RyR2 did not normalize APD prolongation in CREM mice. Our data also revealed that both CREM and CREM:S2814A mice exhibit enhanced $I_{Ca,L}$, which could underlie APD prolongation.[28] Increased $I_{Ca,L}$ and APD prolongation increase the propensity to early afterdepolarizations, which can induce triggered activity and spontaneous ectopy.[29] Thus, early afterdepolarization–mediated processes may underlie the eventual development of atrial ectopy in CREM:S2814A mice, with the protection against ectopy at 3 and 5 months related to suppressed delayed afterdepolarization generation, but further work is needed to directly test this notion. Another candidate mechanism for atrial ectopy in CREM:S2814A mice could be abnormal cardiomyocyte-fibroblast interactions. Fibroblasts can affect electric properties of cardiomyocytes and induce spontaneous automaticity.[30] CREM:S2814A mice developed atrial fibrosis, possibly causing atrial ectopy as a result of abnormal atrial myocyte-fibroblast interactions.

Clinical Relevance

There are presently 2 major challenges for AF treatment. First, AF recurrence is very common; it remains challenging to maintain sinus rhythm in AF patients who undergo cardioversion or AF ablation. Second, up to 15% of initially diagnosed pAF patients will progress to persistent or permanent forms each year.[31]

CaMKII blockers are being developed for clinical use,[32] with the goal of suppressing ectopic atrial activity related to RyR2 hyperphosphorylation that may initiate AF.[2,19] The present findings raise the exciting possibility that such agents may act against AF not only by attacking arrhythmic triggers but also by preventing the Ca^{2+} leak–dependent development of the reentry substrate that underlies progression to more persistent forms. The promise of this approach is underscored by evidence that clinical AF leads to CaMKII hyperphosphorylation of RyR2 and consequent SR Ca^{2+} leak[10] and by our finding in the present study that CREM expression is enhanced in clinical AF (Figure 8), positioning Ca^{2+} leak–induced remodeling as a candidate mechanism for AF progression in humans.

Potential Limitations

The clinical pathophysiology of AF is very complex,[33] and our findings likely do not apply to all clinical forms of AF or to all aspects of AF pathophysiology in any individual patient. We studied a mouse model that has tantalizing similarities to clinical AF in many patients, with the initial presentation of frequent atrial ectopy followed by sAF of progressively longer duration. To the best of our knowledge, this is the only animal

model presenting spontaneous atrial arrhythmias and progression of this type. However, any animal model is limited in the extent to which it mimics clinical AF; therefore, our findings should be extrapolated to humans very cautiously. Moreover, the mechanistic link between the CREM overexpression and CaMKII activation is unknown and requires extensive work in subsequent studies. Nevertheless, our findings that CREM is overexpressed in AF patients and the well-known increase in RyR2 Ca^{2+} leak in clinical AF[7,8,11,34] argue for the potential clinical relevance of our work. These findings provide a potentially important new concept that needs to be evaluated in further experimental and translational studies: that SR Ca^{2+} leak may contribute not only to the spontaneous generation of local triggered activity but also to the development and progression of the AF-maintaining substrate.

Conclusions

RyR2 hyperphosphorylation and SR Ca^{2+} leak are essential mechanisms for the development of sAF in CREM mice. Thus, RyR2 dysfunction can play a role in AF not only as a cause of ectopic trigger activity but also by promoting the AF-maintaining substrate. These findings constitute the first demonstration of molecular mechanisms underlying sAF development in an experimental model, with potentially important pathophysiological and therapeutic implications.

Sources of Funding

This study is supported by grants 09POST2260300 and 12BGIA12050207 (to Dr Li), 12PRE11700012 (to D.Y. Chiang), and 13EIA14560061 (to Dr Wehrens) from the American Heart Association. This work was supported in part by National Heart, Lung, and Blood Institute grants R01-HL089598 and R01-HL091947, the Muscular Dystrophy Association, Fondation Leducq (Alliance for CaMKII Signaling in Heart to Dr Wehrens and European North-American Atrial Fibrillation Research Alliance to Drs Dobrev and Nattel), and DZHK (German Center for Cardiovascular Research; to Dr Dobrev), Deutsche Forschungsgemeinschaft (DFG MU 1376/11-1 to Drs Müller and Schmitz), IZKF Münster (Mü1/014/11 to Drs Müller and Schmitz), Canadian Institutes of Health Research (MGP6957 and MOP44365 to Dr Nattel), and the Heart and Stroke Foundation of Canada (to Dr Nattel). D.Y. Chiang was also supported by the Medical Scientist Training Program Caskey Scholarship. Dr Wehrens holds the Juanita P. Quigley Endowed Chair in Cardiology.

Disclosures

None.

References

1. Naccarelli GV, Varker H, Lin J, Schulman KL. Increasing prevalence of atrial fibrillation and flutter in the United States. *Am J Cardiol*. 2009;104:1534–1539.
2. Dobrev D, Nattel S. New antiarrhythmic drugs for treatment of atrial fibrillation. *Lancet*. 2010;375:1212–1223.
3. Komatsu T, Sato Y, Ozawa M, Kunugita F, Ueda H, Tachibana H, Morino Y, Nakamura M. Relationship between CHADS2 score and efficacy of antiarrhythmic drug therapy in patients with paroxysmal atrial fibrillation. *Circ J*. 2013;77:639–645.
4. Kirchhof P, Marijon E, Fabritz L, Li N, Wang W, Wang T, Schulte K, Hanstein J, Schulte JS, Vogel M, Mougenot N, Laakmann S, Fortmueller L, Eckstein J, Verheule S, Kaese S, Staab A, Grote-Wessels S, Schotten U, Moubarak G, Wehrens XH, Schmitz W, Hatem S, Müller FU. Overexpression of cAMP-response element modulator causes abnormal growth and development of the atrial myocardium resulting in a substrate for sustained atrial fibrillation in mice. *Int J Cardiol*. 2013;166:366–374.
5. Chelu MG, Sarma S, Sood S, Wang S, van Oort RJ, Skapura DG, Li N, Santonastasi M, Müller FU, Schmitz W, Schotten U, Anderson ME, Valderrábano M, Dobrev D, Wehrens XH. Calmodulin kinase II-mediated sarcoplasmic reticulum Ca^{2+} leak promotes atrial fibrillation in mice. *J Clin Invest*. 2009;119:1940–1951.
6. Vest JA, Wehrens XH, Reiken SR, Lehnart SE, Dobrev D, Chandra P, Danilo P, Ravens U, Rosen MR, Marks AR. Defective cardiac ryanodine receptor regulation during atrial fibrillation. *Circulation*. 2005;111:2025–2032.
7. Li N, Wang T, Wang W, Cutler MJ, Wang Q, Voigt N, Rosenbaum DS, Dobrev D, Wehrens XH. Inhibition of CaMKII phosphorylation of RyR2 prevents induction of atrial fibrillation in FKBP12.6 knockout mice. *Circ Res*. 2012;110:465–470.
8. Voigt N, Li N, Wang Q, Wang W, Trafford AW, Abu-Taha I, Sun Q, Wieland T, Ravens U, Nattel S, Wehrens XH, Dobrev D. Enhanced sarcoplasmic reticulum Ca^{2+} leak and increased Na^{+}-Ca^{2+} exchanger function underlie delayed afterdepolarizations in patients with chronic atrial fibrillation. *Circulation*. 2012;125:2059–2070.
9. van Oort RJ, McCauley MD, Dixit SS, Pereira L, Yang Y, Respress JL, Wang Q, De Almeida AC, Skapura DG, Anderson ME, Bers DM, Wehrens XH. Ryanodine receptor phosphorylation by calcium/calmodulin-dependent protein kinase II promotes life-threatening ventricular arrhythmias in mice with heart failure. *Circulation*. 2010;122:2669–2679.
10. Shannon TR, Ginsburg KS, Bers DM. Quantitative assessment of the SR Ca^{2+} leak-load relationship. *Circ Res*. 2002;91:594–600.
11. Gillis AM, Krahn AD, Skanes AC, Nattel S. Management of atrial fibrillation in the year 2033: new concepts, tools, and applications leading to personalized medicine. *Can J Cardiol*. 2013;29:1141–1146.
12. Zou R, Kneller J, Leon LJ, Nattel S. Substrate size as a determinant of fibrillatory activity maintenance in a mathematical model of canine atrium. *Am J Physiol Heart Circ Physiol*. 2005;289:H1002–H1012.
13. Demetrius L. Aging in mouse and human systems: a comparative study. *Ann NY Acad Sci*. 2006;1067:66–82.
14. Morillo CA, Klein GJ, Jones DL, Guiraudon CM. Chronic rapid atrial pacing: structural, functional, and electrophysiological characteristics of a new model of sustained atrial fibrillation. *Circulation*. 1995;91:1588–1595.
15. Willems R, Holemans P, Ector H, Sipido KR, Van de Werf F, Heidbüchel H. Mind the model: effect of instrumentation on inducibility of atrial fibrillation in a sheep model. *J Cardiovasc Electrophysiol*. 2002;13:62–67.
16. Neef S, Dybkova N, Sossalla S, Ort KR, Fluschnik N, Neumann K, Seipelt R, Schöndube FA, Hasenfuss G, Maier LS. CaMKII-dependent diastolic SR Ca^{2+} leak and elevated diastolic Ca^{2+} levels in right atrial myocardium of patients with atrial fibrillation. *Circ Res*. 2010;106:1134–1144.
17. Purohit A, Rokita AG, Guan X, Chen B, Koval OM, Voigt N, Neef S, Sowa T, Gao Z, Luczak ED, Stefansdottir H, Behunin AC, Li N, El Accaoui RN, Yang B, Swaminathan PD, Weiss RM, Wehrens XH, Song LS, Dobrev D, Maier LS, Anderson ME. Oxidized CaMKII triggers atrial fibrillation. *Circulation*. 2013;128:1748–1757.
18. Wehrens XH, Lehnart SE, Reiken SR, Marks AR. Ca^{2+}/calmodulin-dependent protein kinase II phosphorylation regulates the cardiac ryanodine receptor. *Circ Res*. 2004;94:e61–e70.
19. Sood S, Chelu MG, van Oort RJ, Skapura D, Santonastasi M, Dobrev D, Wehrens XH. Intracellular calcium leak due to FKBP12.6 deficiency in mice facilitates the inducibility of atrial fibrillation. *Heart Rhythm*. 2008;5:1047–1054.
20. Shan J, Xie W, Betzenhauser M, Reiken S, Chen BX, Wronska A, Marks AR. Calcium leak through ryanodine receptors leads to atrial fibrillation in 3 mouse models of catecholaminergic polymorphic ventricular tachycardia. *Circ Res*. 2012;111:708–717.
21. Greiser M, Neuberger HR, Harks E, El-Armouche A, Boknik P, de Haan S, Verheyen F, Verheule S, Schmitz W, Ravens U, Nattel S, Allessie MA, Dobrev D, Schotten U. Distinct contractile and molecular differences between two goat models of atrial dysfunction: AV block-induced atrial dilatation and atrial fibrillation. *J Mol Cell Cardiol*. 2009;46:385–394.
22. El-Armouche A, Boknik P, Eschenhagen T, Carrier L, Knaut M, Ravens U, Dobrev D. Molecular determinants of altered Ca^{2+} handling in human chronic atrial fibrillation. *Circulation*. 2006;114:670–680.
23. King JH, Zhang Y, Lei M, Grace AA, Huang CL, Fraser JA. Atrial arrhythmia, triggering events and conduction abnormalities in isolated murine RyR2-P2328S hearts. *Acta Physiol (Oxf)*. 2013;207:308–323.
24. Nattel S, Dobrev D. The multidimensional role of calcium in atrial fibrillation pathophysiology: mechanistic insights and therapeutic opportunities. *Eur Heart J*. 2012;33:1870–1877.
25. Qi XY, Yeh YH, Xiao L, Burstein B, Maguy A, Chartier D, Villeneuve LR, Brundel BJ, Dobrev D, Nattel S. Cellular signaling underlying atrial tachycardia remodeling of L-type calcium current. *Circ Res*. 2008;103:845–854.

26. Luo X, Pan Z, Shan H, Xiao J, Sun X, Wang N, Lin H, Xiao L, Maguy A, Qi XY, Li Y, Gao X, Dong D, Zhang Y, Bai Y, Ai J, Sun L, Lu H, Luo XY, Wang Z, Lu Y, Yang B, Nattel S. MicroRNA-26 governs profibrillatory inward-rectifier potassium current changes in atrial fibrillation. *J Clin Invest*. 2013;123:1939–1951.
27. Pandit SV, Berenfeld O, Anumonwo JM, Zaritski RM, Kneller J, Nattel S, Jalife J. Ionic determinants of functional reentry in a 2-D model of human atrial cells during simulated chronic atrial fibrillation. *Biophys J*. 2005;88:3806–3821.
28. Wehrens XH, Abriel H, Cabo C, Benhorin J, Kass RS. Arrhythmogenic mechanism of an LQT-3 mutation of the human heart Na(+) channel alpha-subunit: a computational analysis. *Circulation*. 2000;102:584–590.
29. Koval OM, Guan X, Wu Y, Joiner ML, Gao Z, Chen B, Grumbach IM, Luczak ED, Colbran RJ, Song LS, Hund TJ, Mohler PJ, Anderson ME. CaV1.2 beta-subunit coordinates CaMKII-triggered cardiomyocyte death and afterdepolarizations. *Proc Natl Acad Sci USA*. 2010;107:4996–5000.
30. Yue L, Xie J, Nattel S. Molecular determinants of cardiac fibroblast electrical function and therapeutic implications for atrial fibrillation. *Cardiovasc Res*. 2011;89:744–753.
31. Camm J. Antiarrhythmic drugs for the maintenance of sinus rhythm: risks and benefits. *Int J Cardiol*. 2012;155:362–371.
32. Savelieva I, Camm J. Anti-arrhythmic drug therapy for atrial fibrillation: current anti-arrhythmic drugs, investigational agents, and innovative approaches. *Europace*. 2008;10:647–665.
33. Iwasaki YK, Nishida K, Kato T, Nattel S. Atrial fibrillation pathophysiology: implications for management. *Circulation*. 2011;124:2264–2274.
34. Voigt N, Heijman J, Wang Q, Chiang DY, Li N, Karck M, Wehrens XH, Nattel S, Dobrev D. Cellular and molecular mechanisms of atrial arrhythmogenesis in patients with paroxysmal atrial fibrillation. *Circulation*. November 18, 2013. doi:10.1161/CIRCULATIONAHA.113.006641. http://circ.ahajournals.org/content/early/2013/11/17/CIRCULATIONAHA.113.006641.long. Accessed November 26, 2013.

CLINICAL PERSPECTIVE

Atrial fibrillation (AF) is commonly characterized by a progressive pattern, moving from spontaneous atrial ectopy to paroxysmal AF and finally to long-standing persistent AF that is often resistant to therapy. The most important obstacle to effective long-term management of AF is the progression of the substrate, as manifested by substantial late AF recurrence rates after initially effective AF ablations. Ultimately, the only way to prevent long-term AF recurrence is to develop effective methods to forestall the molecular mechanisms that lead to substrate progression. The CREM transgenic mouse model of spontaneous AF mimics clinical progression, showing initially isolated atrial ectopy, then repeated bouts of AF, followed by frequent long-lasting AF episodes. We exploited the CREM transgenic mouse to study the molecular basis of AF progression, obtaining evidence that excess calcium leak from the sarcoplasmic reticulum via ryanodine receptor type 2 activates the calcineurin–nuclear factor of activated T cell–Rcan pathway, resulting in atrial dilatation, decreased connexin40 expression, and decreased conduction velocity. Normalization of the ryanodine receptor type 2–mediated calcium leak by crossing CREM transgenic mice with mice having a modified ryanodine receptor type 2 calcium release channel that eliminates calcium leak prevented atrial dilatation, conduction velocity reduction, and AF progression. Thus, our study suggests that ryanodine receptor type 2–mediated sarcoplasmic reticulum calcium leak drives AF progression via the calcineurin–nuclear factor of activated T cell–Rcan system and possibly other remodeling pathways. Our findings present the first clear insights into the molecular mechanisms underlying AF progression and suggest that modulation of ryanodine receptor type 2 may be a novel therapeutic strategy for halting AF development and progression.

Supplemental Material

Supplemental Methods

Human atrial samples. The collection of human tissue samples was approved by the Institutional Review Board of Medical Faculty Mannheim, Heidelberg University (No. 2011–216 N-MA).[1] Right atrial appendages were obtained from 12 sinus rhythm (Ctl) patients, 6 paroxysmal and 4 long-standing persistent (chronic) AF patients undergoing open-heart surgery. Patient characteristics are provided in Supplemental Table S4. All patients gave informed consents.

Study animals. All animal studies were performed according to protocols approved by the Institutional Animal Care and Use Committee of Baylor College of Medicine conforming to the *Guide for the Care and Use of Laboratory Animals* published by the U.S. National Institutes of Health. CREM-IbΔC-X (CREM) transgenic mice were previously established on a FVB/N background[2] and RyR2^{S2814A} (S2814A) knock-in mice were previously established on the C57BL/6 background.[3] In S2814A mice, Serine2814 on RyR2 was substituted with alanine, which inhibits CaMKII phosphorylation of S2814 on RyR2. We intercrossed CREM mice with S2814A mice, to obtain the CREM:S2814A mice. Wild-type (WT), CREM and CREM:S2814A mice on a mixed genetic background were used in the current study.

***Telemetry ECG recordings*.** Mice were implanted with telemeters (Data Sciences International, MN, USA) as previously described.[4] 24-hour ambulatory ECG was monitored in conscious mice at ages of 3, 5 and 7 months. Telemetry ECG recordings were analyzed using ECG-Auto software (emka Technologies). When a mouse exhibited at least one atrial ectopic complex during 24-hour recording, it was considered as atrial ectopy positive. Quantification of spontaneous atrial ectopic events was obtained between 12 p.m. and 1 p.m. to exclude confounding effects of circadian variation. AF was defined by absent P-waves and irregular R-R intervals on telemetry ECG recording for at least 1 second. When a mouse exhibited one

episode of AF longer than 1 second during 24-hour recording, it was considered to show sAF.

Intracardiac electrophysiology in mice. *In vivo* electrophysiology studies were performed in mice at the age of 4-5 months, as previously described.[5] Briefly, atrial and ventricular intracardiac electrograms were recorded using an 1.1F octapolar catheter (EPR-800, Millar Instruments, Houston, Texas) inserted via the right jugular vein. Surface and intracardiac electrophysiology parameters were assessed at baseline. Right atrial pacing was performed using 2-ms current pulses delivered by an external stimulator (STG-3008, Multi Channel Systems, Reutlingen, Germany). AF inducibility was determined by using an overdriving pacing protocol and defined as the occurrence of rapid and fragmented atrial electrograms with irregular AV-nodal conduction and ventricular rhythm for at least 1 second.

***Transthoracic echocardiography*.** Cardiac function was assessed using a VisualSonics VeVo 770 Imaging System (VisualSonics, Toronto, Canada) equipped with high-frequency 30 MHz probe, as described.[6]

***Mouse atrial myocyte isolation*.** Atrial myocytes were isolated by a modified collagenase method as described.[5] Briefly, the heart was removed and the blood was washed out with 0 Ca^{2+} Tyrode solution (137 mM NaCl, 5.4 mM KCl, 1 mM $MgCl_2$, 5 mM HEPES, 10 mM glucose, 3 mM NaOH, pH 7.4). The heart was cannulated through the aorta and perfused on a Langendorff apparatus with 0 Ca^{2+} Tyrode for 3 to 5 minutes at 37 °C, followed by 0 Ca^{2+} Tyrode containing 20 μg/mL Liberase (Roche, Indianapolis, IN) for 10 to 15 minutes at 37 °C. After digestion, heart was perfused with 5 mL KB solution (90 mM KCl, 30 mM K_2HPO_4, 5 mM $MgSO_4$, 5 mM pyruvic acid, 5 mM β-hydroxybutyric acid, 5 mM creatine, 20 mM taurine, 10 mM glucose, 0.5 mM EGTA, 5 mM HEPES, pH 7.2). Both left and right atrium were minced in KB solution and gently agitated, then filtered through a 210 mm polyethylene mesh. Atrial myocytes

were stored in KB solution at room temperature before use.

***Ca^{2+} imaging*.** Atrial myocytes were loaded with 2 μmol/L Fluo-4-AM (Invitrogen, Carlsbad, CA) in normal Tyrode solution containing 1.8 mmol/L Ca^{2+} for 30 minutes at room temperature. Cells were washed with Tyrode solution for 15 minutes for de-esterification and transferred to a chamber equipped with parallel platinum electrodes. For Ca^{2+} sparks recordings, the chamber was placed on a LSM510 confocal microscope (Carl Zeiss, Thornwood, NY). Fluorescence images were recorded in line-scan mode with 1024 pixels per line at 500 Hz. Once steady state Ca^{2+} transient induced by 1Hz-pacing (5 ms, 10 V) was observed, pacing was stopped for 20 seconds and Ca^{2+} sparks were counted using SparkMaster.[7] Steady state SR Ca^{2+} content was estimated by rapid application of caffeine (10mmol/L) after pacing.

Sarcoplasmic reticulum preparation. Atrial tissues were homogenized on ice in a solution containing (in mmol/L) HEPES 10, sucrose 500 and EDTA 5, supplemented with NaF 20, Na_3VO_4 1, and protease inhibitor and phosphatase inhibitor cocktails (cOmplete, Mini and PhosSTOP from Roche Applied Science, Indianapolis, IN). The samples were subsequently subjected to three steps of centrifugation: 1) 3,800 g for 15 min at 4 °C; 2) the supernatants from step 1 were collected and centrifuged at 27,900 g for 15 min at 4 °C; 3) the supernatants from step 2 were ultracentrifuged at 110,000 g for 1 hour at 4 °C. The supernatants from step 3 were discarded while the pellets were resuspended in 50 μl of the same solution as for homogenization but without the EDTA. The resultant suspensions were used for single channel recording.

Single-channel recordings of RyR2 channels. Single-channel recordings were obtained under voltage-clamp conditions at 0 mV, as previously described.[8] Atrial SR membrane-

preparations were incorporated into lipid-bilayer membranes comprised of a mixture of phosphatidylethanolamine and phosphatidylserine at a ratio of 3:1 (Avanti Polar Lipids, Alabaster, AL) dissolved in n-decane (25 mg/mL). Bilayers were formed across a 150 μm aperture of a polystyrene cuvette. The *cis* and *trans* chambers correspond to the cytosolic and the luminal sides of the SR, respectively. The *trans* chamber contained (in mmol/L) HEPES 250, KCl 50 and $CaOH_2$ 53. The *cis* chamber contained (in mmol/L) HEPES 250, Tris-base 125, KCl 50, EGTA 1, $CaCl_2$ 0.35, pH=7.35. Data were collected using Digidata 1322A (Molecular Devices, Sunnyvale, CA) and Warner Bilayer Clamp Amplifier BC-535 (Warner Instruments, Hamden, CT) under voltage-clamp conditions. Data were analyzed from digitized current recordings using pCLAMP-9.2 software (Molecular Devices).

***Optical mapping*.** Optical mapping of action potentials in the mouse atria was performed in mice at the age of 3-5months as previously described.[3] Hearts were rapidly removed and retrogradely perfused with oxygenated Tyrode's solution (containing (mM): 137 NaCl, 5.4 KCl, 1 MgCl2, 2 NaH2PO4, 10 HEPES, 10 glucose, pH adjusted to 7.4 with NaOH) containing 1.2 mM CaCl2 at 37°C in a Langendorff apparatus. The perfusion pressure was maintained constant at ~60-65 mmHg and monitored using an in-line physiological pressure transducer connected to a Bridge Amplifier (AD Instruments Inc). To prevent motion artifacts, blebbistatin at a final concentration of 5 μmol/L was applied as an excitationcontraction uncoupler. The heart was then stained with the voltage-sensitive dye RH237 (0.33 μM) for 10 minutes to monitor changes in membrane potential. After staining, atria were cut and imaged in a chamber perfused with Tyrode containing 1.2 mM CaCl2. Green light (520±20nm) from a 532 nm laser light source (B&W TEK Inc) was shone directly onto the atrial tissue. Emitted fluorescence was collected using electron-multiplying CCD camera (Cascade 128+, Photometrics) covering the same mapped field. A grid was used to calibrate the field of view of the CCD camera. For membrane

voltage, passed fluorescence was collected through a 710 nm long pass filter.

Whole cell patch clamp. L-type Ca^{2+} currents were recorded using the patch clamp technique in the whole-cell configuration. Patch pipettes were pulled on a horizontal Flaming Brown micropipette puller (P-87, Sutter Instruments, Inc.) and the tips were coated with wax (KERR Sticky Wax). When filled with pipette solution, the resistance of the patch pipettes was in a range of 3-5 MΩ. Pipette solution contained (in mM): 140 NMDG, 20 HEPES, 5 EGTA, 10 HCl. The bath solution contained (in mM): 130 TEAOH, 1 $MgCl_2$, 10 HEPES, 10 $CaCl_2$. The pH of the solutions was adjusted to 7.2 with MES. Experiments were performed at room temperature (20-22^{o}C). Data were acquired with an Axopatch 200B amplifier (Molecular Devices). Currents were subsequently filtered by an 8-pole Bessel filter (Frequency Device, Inc.) at 5 kHz and sampled at 200 kHz with an 18-bit A/D converter (Instrutech ITC-18). A P/8 protocol was used for leak subtraction with a holding potential of -100 mV. Data were digitally filtered at 1 kHz during analysis with Igor Pro (WaveMetrics, Inc.).

Western blotting. Western blot analysis was performed in atrial samples of study animals at the ages of 1 month (no atrial arrhythmias), 3 months (atrial ectopy prior to the onset of spontaneous AF), and 7 months (long-lasting spontaneous AF). Protein extraction and western blotting was performed as previously described.[5] Briefly, mouse atrial lysates were subjected to electrophoresis on 5% (for RyR2) and 10 or 12% (for other proteins) acrylamide gels, and transferred onto polyvinyl difluoride membranes. Membranes were probed with mouse anti-RyR2 (1:5,000, #MA3-916, ABR), mouse anti-Thr287-phosphorylated CaMKII (1:1,000, #10011438, Cayman Chemical), rabbit anti-CaMKIIδ (1:1,000, #S2169, Epitomics), rabbit anti-Thr17-phosphorylated PLN (1:5000, #A010-13, Badrilla), mouse anti-PLN (1:5,000, #MA3-922, Pierce), rabbit anti-Cx40 (1:1,000, #AB1726, Millipore), and mouse anti-GAPDH (1:10,000, #MAB-374, Millipore) antibodies at room temperature. The rabbit anti-Ser2808-RyR2 (1:1,000)

and anti-Ser2814-RyR2 (1:1,000) phosphoepitope-specific antibody were custom generated using the peptide C-RTRRI-(pS)-QTSQV corresponding to the PKA phosphorylation site region at serine 2808 on RyR2 and peptide CSQTSQV-(pS)-VD corresponding to RyR2 CaMKII phosphorylated at serine 2814, respectively. Membranes were then incubated with secondary anti-mouse and anti-rabbit antibodies conjugated to Alexa-Fluor 680 (Invitrogen Molecular Probes) and IR800Dye (Rockland Immunochemicals), respectively, and bands were quantified using Image J.

***Histology*.** Whole hearts were excised, washed briefly in normal saline, blotted dry and then fixed in 4% buffered formaldehyde for 48h. Longitudinal 5μm sections were stained with Masson-Trichrome for fibrosis. Fibrosis were quantified as previously described.[9]

***Statistical analysis*.** Continuous variables are presented as mean±SEM and categorical data are presented as percentages. Statistical analysis was performed using SPSS Statistics (IBM, USA). One-way ANOVA followed by the post-hoc Bonferroni t-test was applied for multiple group non-repeated measures data and paired t-test for single repeated measures. Fisher's exact test was used to compare categorical data. To compare continuous variables with a skewed distribution, the Mann-Whitney test was applied. $P<0.05$ was considered statistically significant.

Supplemental Tables

Table S1. Characteristics of Ca^{2+} sparks

	WT (n=157)	CREM (n=360)	CREM:S2814A (n=228)
Amplitude (F/F0)	0.23 ± 0.01	0.27 ± 0.004***	0.25 ± 0.01#
FWHM	1.52 ± 0.05	1.46 ± 0.03	1.56 ± 0.04#
FDHM	17.2 ± 0.5	27.8 ± 0.7***	21.1 ± 0.6###
Full Width	2.48 ± 0.09	2.30 ± 0.06	2.7 ± 0.09###
Full Duration	35.2 ± 1.3	48.0 ± 1.3***	42.3 ± 1.5##
TdP	12.4 ± 0.5	15.8 ± 0.6***	14.0 ± 0.6#
Dvdt	26.3 ± 0.8	27.0 ± 0.4	28.3 ± 0.9
tau	15.9 ± 0.8	32.2 ± 1.3***	20.2 ± 0.9###

FWHM: Full width at half maximum of full width; FDHM: Full duration at half maximum.

*P<0.05, **P<0.01, ***P<0.001 vs WT; #P<0.05, ##P<0.01, ###P<0.001 vs CREM.

Table S2. Cardiac electrophysiological parameters at the age of 5 months.

	WT (n=7)	CREM (n=12)	CREM:S2814A (n=12)
HR (bpm)	622 ± 14	598 ± 18	602 ± 17
PR (ms)	33.9 ± 1.5	43.9 ± 1.0*	39.8 ± 1.3#
QRS (ms)	9.8 ± 0.2	10.1 ± 0.3	10.2 ± 0.4
QTc (ms)	26.6 ± 2.4	27.0 ± 0.7	28.2 ± 0.7
cSNRT (ms)	9.2 ± 1.4	13.4 ± 2.6	12.5 ± 4.5
AVERP (ms)	48.7 ± 1.4	48.0 ± 1.6	48.2 ± 1.8
AERP (ms)	38.2 ± 1.1	33.5 ± 1.9	37.6 ± 2.1

*P<0.05 vs WT; #P<0.05 vs CREM

Table S3. Echocardiographic parameters of WT, CREM, and CREM:S2814A mice at 3 and 5 months of age.

	3 months			5 months		
	WT (n=9)	CREM (n=9)	CREM:S2814A (n=7)	WT (n=7)	CREM (n=6)	CREM:S2814A (n=10)
HR (bpm)	483.9±15.7	501.3±14.6	486.9±21.2	477.1±12.3	455.7±16.6	463.0±14.9
EF (%)	59.0±1.5	54.6±1.9	59.3±1.8	57.9±2.7	61.2±1.9	56.0±1.7$^{\#\#}$
FS (%)	31.0±1.0	28.1±1.2	31.1±1.2	30.3±1.8	32.6±1.4	28.9±1.1$^{\#\#}$
$LVAW_d$ (mm)	0.72±0.04	0.77±0.04	0.69±0.03	0.76±0.02	0.76±0.03	0.79±0.03
$LVID_d$ (mm)	4.08±0.07	4.21±0.11	3.96±0.04	4.11±0.14	4.14±0.11	4.03±0.08
$LVPW_d$ (mm)	0.61±0.03	0.61±0.01	0.57±0.02*	0.60±0.03	0.60±0.04	0.62±0.03
$LVAW_s$ (mm)	0.98±0.06	1.01±0.04	1.05±0.05	1.07±0.04	0.97±0.08	0.92±0.05*
$LVID_s$ (mm)	2.82±0.07	3.04±0.12	2.74±0.04	2.87±0.12	2.69±0.07	2.85±0.11$^{\#}$
$LVPW_s$ (mm)	0.93±0.05	0.90±0.03	0.92±0.05	0.88±0.04	0.94±0.04	0.95±0.05

Data are expressed as mean ± SEM. *P<0.05 vs WT, and $^{\#}$P<0.05, $^{\#\#}$P<0.01 vs CREM. BW= body weight; HR = heart rate; EF = ejection fraction; FS = left ventricular fractional shortening; LVAW = left ventricular anterior wall thickness; LVPW = left ventricular posterior wall thickness. Subscript letters represent during diastole or systole.

Table S4. Characteristics of patients.

	Ctl	pAF	cAF
Patients, n	12	6	4
Gender, M/F	8/4	3/3	4/0
Age, y	67.6 ± 2.2	76.7 ± 2.4*	66.8 ± 0.2
Body mass index, kg/m^2	29.2 ± 1.1	26.7 ± 1.6	29.3 ± 1.1
CAD, n	9	3	4
MVD/AVD, n	0	1	0
CAD+MVD/AVD, n	3	2	0
Hypertension, n	10	5	2
Diabetes, n	2	0	0
Hyperlipidemia, n	8	3	2
LVEF, %	53.3 ± 4.4	53.3 ± 4.1	50.8 ± 6.6
Digitalis, n	1	1	2
ACE inhibitors, n	8	3	3
AT1 blockers, n	1	0	0
β-Blockers, n	8	5	3
Dihydropyridines, n	3	3	1
Diuretics, n	3	3	2
Nitrates, n	1	2	1
Lipid-lowering drugs, n	9	3	2

Ctl, control patients in sinus rhythm; pAF, paroxysmal atrial fibrillation; cAF, chronic atrial fibrillation; CAD, coronary artery disease; MVD/AVD, mitral/aortic valve disease; LVEF, left ventricular ejection fraction; ACE, angiotensin-converting enzyme; AT, angiotensin receptor. *P<0.05 vs Ctl from unpaired Student's *t*-test for continuous variables and from Fisher's exact test for categorical variables.

Supplemental References

1. Voigt N, Heijman J, Wang Q, Chiang DY, Li N, Karck M, Wehrens XH, Nattel S, Dobrev D. Cellular and Molecular Mechanisms of Atrial Arrhythmogenesis in Patients With Paroxysmal Atrial Fibrillation. *Circulation*. 2013 Nov 18. [Epub ahead of print]
2. Muller FU, Lewin G, Baba HA, Boknik P, Fabritz L, Kirchhefer U, Kirchhof P, Loser K, Matus M, Neumann J, Riemann B, Schmitz W. Heart-directed expression of a human cardiac isoform of cAMP-response element modulator in transgenic mice. *J Biol Chem*. 2005;280:6906-6914.
3. Chelu MG, Sarma S, Sood S, Wang S, van Oort RJ, Skapura DG, Li N, Santonastasi M, Muller FU, Schmitz W, Schotten U, Anderson ME, Valderrabano M, Dobrev D, Wehrens XH. Calmodulin kinase II-mediated sarcoplasmic reticulum Ca2+ leak promotes atrial fibrillation in mice. *The Journal of clinical investigation*. 2009;119:1940-1951.
4. van Oort RJ, McCauley MD, Dixit SS, Pereira L, Yang Y, Respress JL, Wang Q, De Almeida AC, Skapura DG, Anderson ME, Bers DM, Wehrens XH. Ryanodine receptor phosphorylation by calcium/calmodulin-dependent protein kinase II promotes life-threatening ventricular arrhythmias in mice with heart failure. *Circulation*. 2010;122:2669-2679.
5. Li N, Wang T, Wang W, Cutler MJ, Wang Q, Voigt N, Rosenbaum DS, Dobrev D, Wehrens XH. Inhibition of CaMKII phosphorylation of RyR2 prevents induction of atrial fibrillation in FKBP12.6 knockout mice. *Circ Res*. 2012;110:465-470.
6. Respress JL, van Oort RJ, Li N, Rolim N, Dixit SS, deAlmeida A, Voigt N, Lawrence WS, Skapura DG, Skardal K, Wisloff U, Wieland T, Ai X, Pogwizd SM, Dobrev D, Wehrens XH. Role of RyR2 phosphorylation at S2814 during heart failure progression. *Circulation research*. 2012;110:1474-1483.

7. Picht E, Zima AV, Blatter LA, Bers DM. SparkMaster: automated calcium spark analysis with ImageJ. *Am J Physiol Cell Physiol*. 2007;293:C1073-1081.

8. Voigt N, Li N, Wang Q, Wang W, Trafford AW, Abu-Taha I, Sun Q, Wieland T, Ravens U, Nattel S, Wehrens XH, Dobrev D. Enhanced sarcoplasmic reticulum Ca2+ leak and increased Na+-Ca2+ exchanger function underlie delayed afterdepolarizations in patients with chronic atrial fibrillation. *Circulation*. 2012;125:2059-2070.

9. Dahab GM, Kheriza MM, El-Beltagi HM, Fouda AM, El-Din OA. Digital quantification of fibrosis in liver biopsy sections: description of a new method by Photoshop software. *J Gastroenterol Hepatol*. 2004;19:78-85.

Supplemental Figures

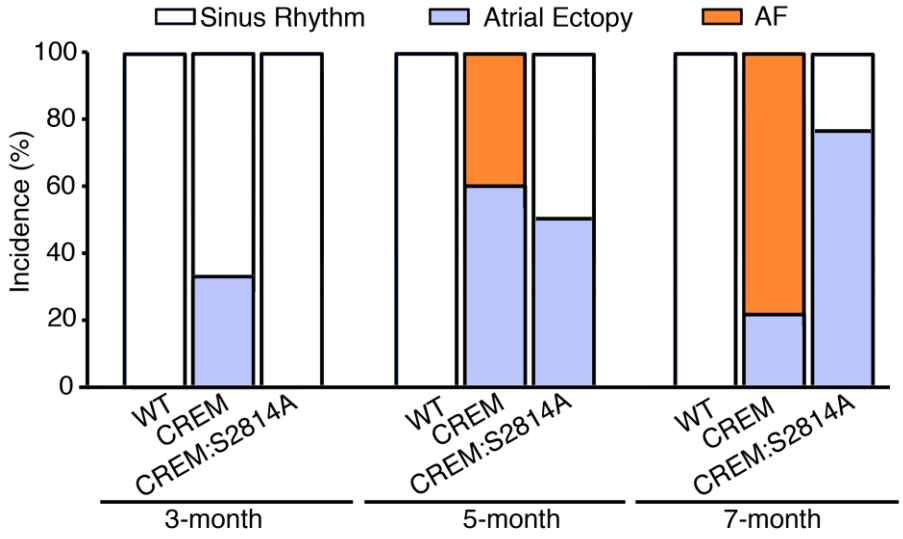

Figure S1. Stacked bar graphs summarizing the incidence of spontaneous atrial ectopy and AF in WT, CREM and CREM:S2814A mice at 3 different ages.

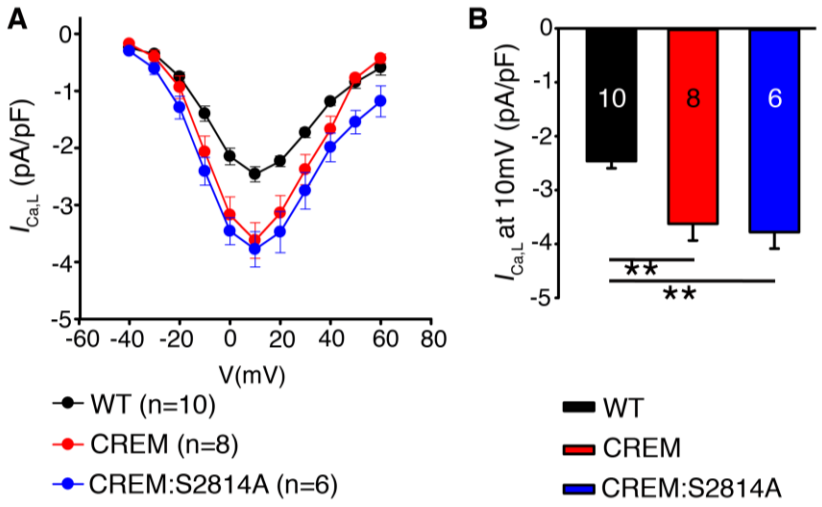

Figure S2. Enhanced L-type Ca^{2+} currents in atrial myocytes**. A.** Current-voltage relationships of $I_{Ca,L}$ obtained in atrial myocytes from WT, CREM and CREM:S2814A. **B.** The peak amplitude of $I_{Ca,L}$ obtained at 10mV. Numbers in the graph indicated number of cells studied from 3-4 mice in each group. **P<0.01.

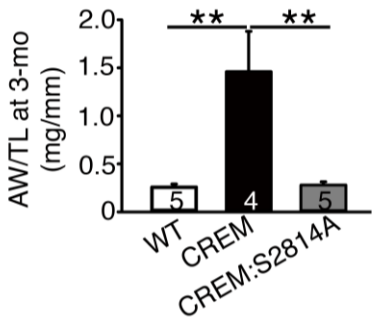

Figure S3. Increased AW/TL in CREM mice at the age of 3 months. **P<0.01.

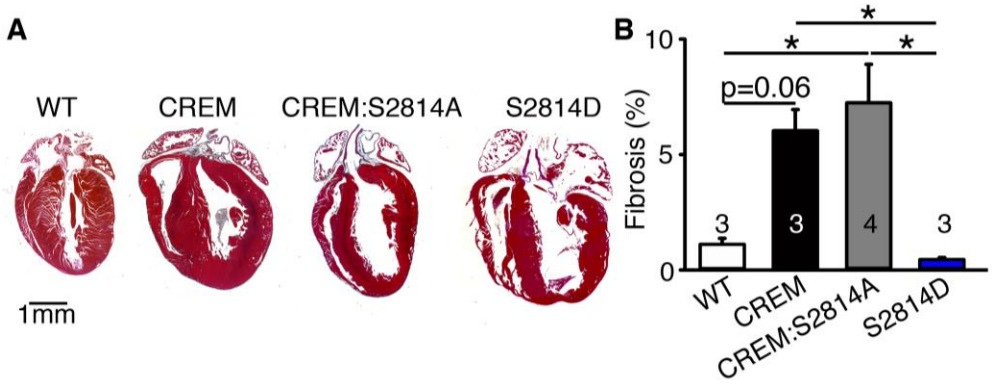

Figure S4. Increased fibrosis in CREM and CREM:S2814A mice. **A.** Masson-Trichrome staining of fibrosis in longitudinal sections. **B.** Quantification of ventricular fibrosis**.** Numbers in the bars indicate the number of animals studied. *P<0.05.